photonics

MDPI

Article

Link-Blockage Model and AP-Placement Scheme for No-Blockage Link between AGV and AP in Logistics–Warehousing VLC Network

Guiyu Gong, Chaoqin Gan *, Yong Fang, Yifan Zhu and Qiuyue Hu

Key Laboratory of Specialty Fiber Optics and Optical Access Networks, Joint International Research Laboratory of Specialty Fiber Optics and Advanced Communication, Shanghai University, Shanghai 200444, China
* Correspondence: cqgan@shu.edu.cn

Abstract: In this paper, the blockage problem of the optical link between AGV (autonomous ground vehicles) and AP (access point) in the logistics–warehousing VLC (visible light communication) network is analyzed. First, based on the random geometric model, a link-blockage model is proposed. Given the position of AGV, AP and obstacle, the blockage state of the VLC link between AGV and AP can be obtained through this model. Then, an AP-placement scheme based on the link-blockage model is proposed. Under this AP placement, AGVs in any position have a reliable link that is not affected by obstacles. During the movement of AGV, the VLC link of AGV will not be interrupted by a random blockage. Finally, the effectiveness of the link-blockage model is demonstrated by the shadow method. In this paper, the link outage probability and the data rate under different AP heights, AP spacings and the number of obstacles are simulated. Simulation results show that the VLC link can keep uninterrupted under the AP placement proposed in this paper.

Keywords: logistics–warehousing; VLC; AGV; link blockage; AP placement

Citation: Gong, G.; Gan, C.; Fang, Y.; Zhu, Y.; Hu, Q. Link-Blockage Model and AP-Placement Scheme for No-Blockage Link between AGV and AP in Logistics–Warehousing VLC Network. *Photonics* **2023**, *10*, 31. https://doi.org/10.3390/photonics10010031

Received: 14 November 2022
Revised: 8 December 2022
Accepted: 23 December 2022
Published: 27 December 2022

1. Introduction

Visible light communication (VLC) is short-range optical communication technology. It provides reliable and low-latency connections, and it is immune to electromagnetic interference [1]. Therefore, VLC has always been a concern for people. At the same time, wireless communication is becoming a key technology for logistics–warehousing automation. AGVs are called autonomous ground vehicles. It has great application potential in logistics warehouses [2,3].

It is very promising to use VLC to realize the wireless communication of AGV [4]. In the logistics warehouse, communication between the receiver on the AGV and the VLC access point (AP) deployed on the ceiling is realized through a line-of-sight (LOS) link. It is necessary to have an uninterrupted link [5]. Current research on link blockage mainly focuses on the blockage caused by the human body. Singh A analyzed the downlink performance of an indoor VLC system with static human blockage [6]. A. A. Okine approximated the shape of the human body as a cube and a cylinder and derived the closed expression of blockage time and angle [7]. Tang Tang investigated the impact of multiple shadows on indoor VLC systems composed of a VLC AP and multiple terminals [8]. J. Beysens considered the blockage effect of users themselves on LOS links and designed a novel user-in-the-loop mechanism [9]. A hybrid LiFi and WiFi network is proposed to resist link blockage [10]. The performance of a single static user under the influence of random device orientation and link blockage was studied in [11]. The blockage model proposed in the above research is not suitable for the VLC link between AGV and AP. In logistics warehouses, the VLC link is easily blocked by shelves and mobile AGVs carrying the shelf. Therefore, in order to realize a reliable connection, it is very important to analyze the blockage problem of VLC links.

In this paper, link blockage between AGV and VLC AP is studied. The link-blockage model for the VLC link between AGV and AP is first proposed. Based on the link-blockage model, this paper proposes an AP-placement scheme to achieve uninterrupted links during AGV movement.

2. System Model

2.1. Channel Model

This paper considers the downlink of the LOS link. The VLC AP on the ceiling is the transmitter, and the receiver is on the AGV. For indoor VLC networks, the channel model is assumed to be Lambertian radiation. The channel gain is given by [12]:

$$H_{i,j} = \begin{cases} \frac{(m+1)A}{2\pi d_{i,j}^2} cos^m(\phi) g_f g(\psi) cos(\psi), 0 \le \psi \le \Psi_c \\ 0, \psi > \Psi_c \end{cases} \quad (1)$$

Among them, A represents the effective receiving area of the receiver. g_f is the gain of the optical filter. m is the Lambertian order ($m = -1/\log_2 cos(\Phi_{1/2})$). $\phi_{1/2}$ is half-intensity angle. $\phi(\phi \in [0, \Phi_{1/2}])$ represents the radiance angle of the transmitter. ψ represents the incidence angle of the receiver. $g(\psi)$ is the optical concentrator gain ($g(\psi) = \zeta^2/(sin\Psi_c)^2$). ζ is the refractive index. Ψ_c is the receiver field of view (FOV). $d_{i,j}$ represents the distance between the $j-th$ transmitter and the $i-th$ receiver ($d_{i,j} = \sqrt{L^2 + r^2}$). L, r is the vertical and horizontal distance between the transmitter and receiver, respectively.

To reflect the influence of link blockage on the LOS link, an indicator function $b_{i,j}$ is defined as $b_{i,j} = \begin{cases} 1, if\ LOS\ link\ is\ not\ blocked \\ 0, if\ LOS\ link\ is\ blocked \end{cases}$. The reliability of the communication system is usually measured by the signal-to-noise ratio. The signal-to-noise ratio (SNR) is the ratio of signal power and noise power received by the receiver. By considering link blockage, the SNR of the VLC channel is given by [8]:

$$SNR_{i,j} = \frac{\left(R_{PD} P H_{i,j} b_{i,j}\right)^2}{NB} \quad (2)$$

Among them, R_{PD} represents is the responsivity of the photodetector. P represents the transmitted optical power. B is the bandwidth. N is the spectral density of the additive white Gaussian noise (AWGN).

2.2. Metrics of Channel Reliability

The outage probability and data rate are selected as metrics of channel reliability in this paper. The expression of the available data rate is [8]:

$$R_{i,j} = B\log_2\left(1 + \frac{1}{2\pi e} SNR_{i,j}\right) \quad (3)$$

Among them, e is a constant, and the value is 2.71828. The expression of the outage probability is [8]:

$$OP = \Pr\{SNR_{i,j} \le \gamma_o\} \quad (4)$$

Among them, γ_o represents the minimum threshold of SNR that meets the communication requirements. In this paper, the value of γ_o is 20 dB.

3. Link-Blockage Model

This paper mainly studies the wireless link of the AGV using visible light communication. AGVs are mainly used in logistics warehouses to achieve the functional requirements of item-to-person picking. The working environment of AGV is composed of two parts: shelves and road, as shown in Figure 1. The shelf height is much higher than that of the AGV. The VLC AP is deployed on the ceiling. The AGV moves along the central axis of the

road. In the logistics–warehousing VLC network, the shelves and the AGV carrying goods block the VLC link easily. In industrial applications, it is very important to realize wireless communication with high reliability. Therefore, achieving no blockage is very critical for the VLC link of the AGV. In this paper, AGV carrying goods is called a dynamic obstacle. The shelf is called a static obstacle. These cubes are used to simulate obstacles. The receiver is in the middle of the AGV. The height of AP is H_l. The body size of AGV is $L_g * W_g * H_g$. The shelf size is $L_O * W_O * H_O$. The width of the road is W_R. The size of the static obstacles is the same as that of the dynamic obstacles. P_g represents the position of the receiver on the AGV. The coordinate of the receiver is $P_g = (x_g, y_g, H_g)$. The coordinate of the AP is $P_l = (x_l, y_l, H_l)$. The coordinate of the obstacle is $P_o = (x_o, y_o, H_o + H_g)$.

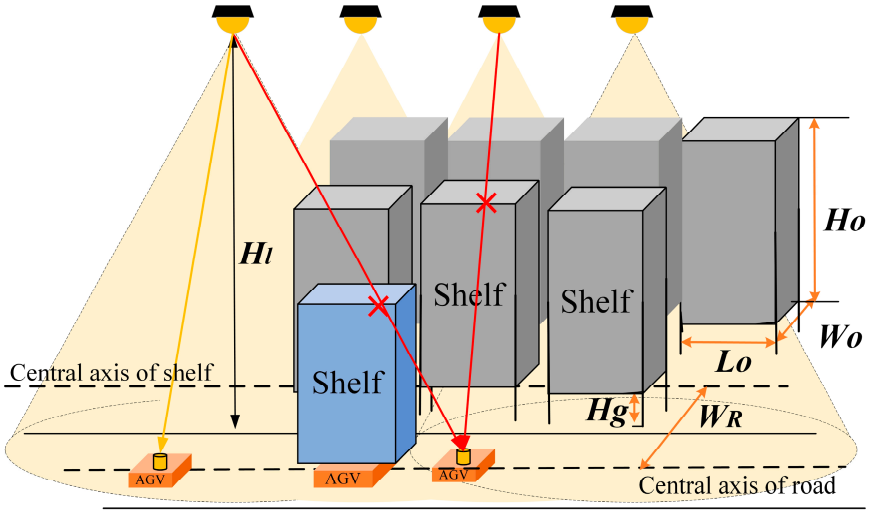

Figure 1. Blocking source of VLC link between AGV and AP.

3.1. Link Blockage Caused by Static Obstacle

Shelves on both sides of the road may block the VLC link. In this paper, D_{go} represents the horizontal distance between the receiver of AGV and the obstacle. D_{gl} represents the horizontal distance between the receiver of AGV and the AP. P_b represents the blocking point of the VLC link. D_{gb} represents the horizontal distance between the receiver and the p_b. As can be seen from Figure 2a, the threshold value of D_{gb} is $D_{gb}^{thr} = \frac{H_O D_{gl}}{H_l - H_g}$.

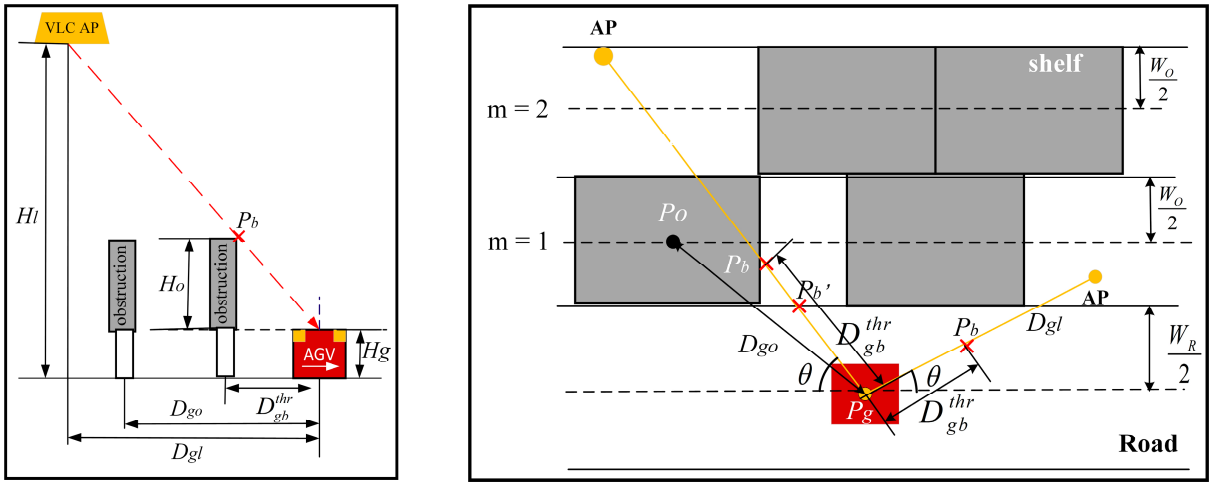

Figure 2. Analysis of link blockage caused by static obstacle: (**a**) horizontal view; (**b**) top view.

If the VLC link has an intersection with the obstacle and the horizontal distance from the intersection to the AGV is less than D_{gb}^{thr}, the VLC link will be blocked. In this paper, the angle between the projection of the VLC link and the center axis of the road is represented by $\theta(\theta \in [0, \frac{\pi}{2}])$. W_O represents the width of the obstacle. L_O represents the length of the obstacle. It can be seen from Figure 2b that when $D_{gb}^{thr} sin\theta \leq \frac{W_R}{2}$, the blocking points are inside the road. In this case, the VLC link is not affected by static obstacles.

D_{go}^{pro} represents the component of D_{go} on the central axis of the road. That is, $D_{go}^{pro} = \sqrt{{D_{go}}^2 - \left[\frac{(W_R + (2m-1)W_O}{2}\right]^2}$. m represents the $m-th$ row of shelf. When $D_{gb}^{thr} sin\theta > \frac{W_R}{2}$, there will be three situations.

If $(x_l - x_g) = 0\ or\ (y_l - y_g) = 0$, the link will be blocked by static obstacles when $D_{go}^{pro} \leq \frac{L_O}{2}$. If $(x_l - x_g)(x_o - x_g) > 0\ or\ (y_l - y_g)(y_o - y_g) > 0$, the AP and the obstacle are on the same side of the AGV. In this case, if $\min\left\{\left|D_{gb}^{thr} cos\theta - D_{go}^{pro}\right|, \left|\frac{W_R}{2tan\theta} - D_{go}^{pro}\right|\right\} \leq \frac{L_O}{2}$, the link will be blocked by static obstacles. If $(x_l - x_g)(x_o - x_g) < 0\ or\ (y_l - y_g)(y_o - y_g) < 0$, the AP and the obstacle are on different sides of the AGV. In this case, if $\left|\frac{W_R}{2tan\theta} + D_{go}^{pro}\right| \leq \frac{L_O}{2}$, the link will be blocked by static obstacles.

In this paper, $\gamma_s\{0, 1\}$ represents the blockage state of the VLC link caused by static obstacles. $\gamma_s = 1$ means the link is blocked by static obstacles. $\gamma_s = 0$ means the link is not blocked by static obstacles. Therefore, the occurrence conditions of link blockage caused by static obstacles are:

$$\gamma_s = \begin{cases} 1, when \begin{cases} D_{gl} sin\theta > \frac{W_R(H_l - H_g)}{2H_O} \\ (x_l - x_g)(x_o - x_g) > 0\ or\ (y_l - y_g)(y_o - y_g) > 0 \\ \min\left\{\left|D_{gb}^{thr} cos\theta - D_{go}^{pro}\right|, \left|\frac{W_R}{2tan\theta} - D_{go}^{pro}\right|\right\} \leq \frac{L_O}{2} \end{cases} \\ 1, when \begin{cases} D_{gl} sin\theta > \frac{W_R(H_l - H_g)}{2H_O} \\ (x_l - x_g)(x_o - x_g) < 0\ or\ (y_l - y_g)(y_o - y_g) < 0 \\ \left|\frac{W_R}{2tan\theta} + D_{go}^{pro}\right| \leq \frac{L_O}{2} \end{cases} \\ 1, when \begin{cases} D_{gl} sin\theta > \frac{W_R(H_l - H_g)}{2H_O} \\ (x_l - x_g) = 0\ or\ (y_l - y_g) = 0 \\ D_{go}^{pro} \leq \frac{L_O}{2} \end{cases} \\ 0, others \end{cases} \tag{5}$$

3.2. Link Blockage Caused by Dynamic Obstacle

AGVs carrying goods may block the VLC link. It can be seen from Figure 3 that the blocking situation can be divided into three types. When $D_{gb}^{thr} sin\theta \leq \frac{W_O}{2}$, if $(x_l - x_g)(x_o - x_g) > 0\ or\ (y_l - y_g)(y_o - y_g) > 0$ and $D_{gb}^{thr} cos\theta \geq \left|D_{go} - \frac{L_O}{2}\right|$, the VLC link will be blocked by dynamic obstacles. When $D_{gb}^{thr} sin\theta > \frac{W_O}{2}$, the critical blocking point should be $P_{b\prime}$. In this case, if $(x_l - x_g)(x_o - x_g) > 0\ or\ (y_l - y_g)(y_o - y_g) > 0$ and $\left|D_{go} - \frac{L_O}{2}\right| \leq \frac{W_O}{2tan\theta}$ the VLC link will be blocked by dynamic obstacles. If $(x_l - x_g) = 0\ or\ (y_l - y_g) = 0$, the VLC link is not affected by dynamic obstacles.

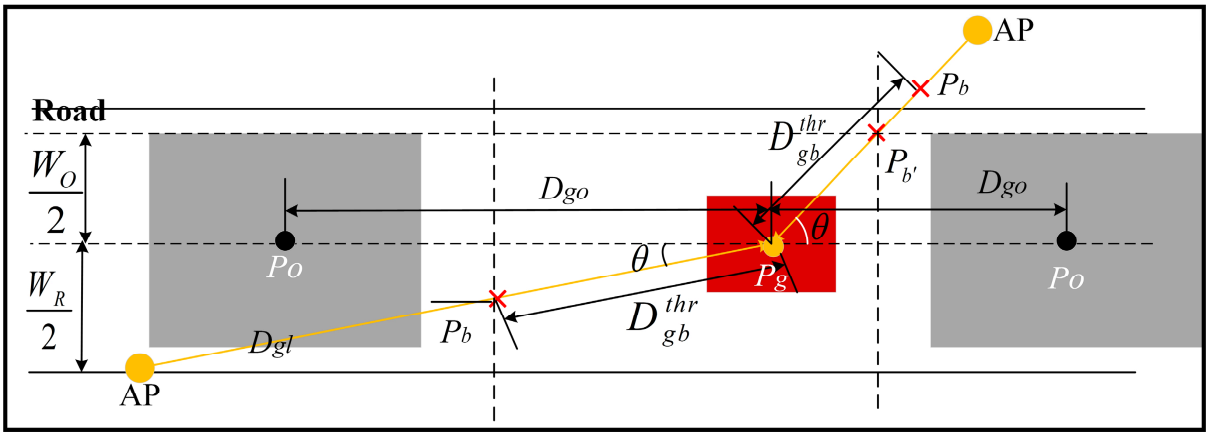

Figure 3. Analysis of link blockage caused by dynamic obstacle.

In this paper, $\gamma_d\{0,1\}$ represents the blockage state of the VLC link caused by dynamic obstacles. $\gamma_d = 1$ means the link is blocked by a dynamic obstacle. $\gamma_d = 0$ means the link is not blocked by a dynamic obstacle. Therefore, the occurrence conditions of link blockage caused by dynamic obstacles are:

$$\gamma_d = \begin{cases} 1, when \begin{cases} D_{gl} sin\theta \le \frac{W_O(H_l - H_g)}{2H_O} \\ D_{gl} cos\theta \ge \frac{(H_l - H_g)}{H_O} \left| D_{go} - \frac{L_O}{2} \right| \\ (x_l - x_g)(x_o - x_g) > 0 \; or \; (y_l - y_g)(y_o - y_g) > 0 \end{cases} \\ 1, when \begin{cases} D_{gl} sin\theta > \frac{W_O(H_l - H_g)}{2H_O} \\ \frac{W_O}{2tan\theta} \ge \left| D_{go} - \frac{L_O}{2} \right| \\ (x_l - x_g)(x_o - x_g) > 0 \; or \; (y_l - y_g)(y_o - y_g) > 0 \end{cases} \\ 0, others \end{cases} \tag{6}$$

3.3. Link Blockage Caused by Static Obstacle and Dynamic Obstacle

When one of the static blockage and dynamic blockage is met, the VLC link will be blocked. In this paper, $\gamma\{1,0\}$ represent the blockage state of the VLC link. $\gamma = 1$ means the link is blocked. $\gamma = 0$ means the link is not blocked. Therefore, the occurrence conditions of link blockage are:

$$\gamma = \begin{cases} 0, \gamma_d = 0 \; and \; \gamma_s = 0 \\ 1, others \end{cases} \tag{7}$$

Thus far, the link-blockage model for the VLC link between the AGV and the AP has been established. Given the position of AGV, AP and obstacle, the link state between AGV and AP can be obtained through this model.

4. The AP-Placement Scheme for No-Blockage Link between AGV and VLC AP

In the logistics–warehousing VLC network, the VLC link between the AGV and the AP is easily blocked. However, industrial applications have high requirements for link reliability. Therefore, it is important to ensure that AGV has a no-blockage link by deploying APs reasonably.

4.1. Analysis of Link-Blockage Model

When the receiver is deployed in the middle of the AGV, the minimum horizontal distance between the static obstacle and the receiver is $\frac{W_R}{2} + \frac{W_O}{2}$. The minimum horizontal distance between the dynamic obstacle and the receiver is $\frac{L_g}{2} + \frac{L_O}{2}$. Next, the receiver on the AGV is used as a reference point. The distance between different obstacles and the receiver is set as the minimum value. Under the influence of different obstacles, the link

status of APs in different areas is analyzed. The sides of the road are symmetrical. The link analysis before and after the AGV is consistent. Therefore, it is enough to analyze the AP area of one quadrant.

According to Equation (5), the AP area can be divided into three parts when $D_{go} = \frac{W_R}{2} + \frac{W_O}{2}$. When $D_{gl}sin\theta \leq \frac{W_R(H_l - H_g)}{2H_O}$, the link is not affected by static obstacles, as shown at (1) in Figure 4a. When $D_{gl}sin\theta > \frac{W_R(H_l - H_g)}{2H_O}$ and $tan\theta \geq \frac{w_R}{L_O}$, the VLC link will be blocked by static obstacles, as shown at (2) in Figure 4a. When $D_{gl}sin\theta > \frac{W_R(H_l - H_g)}{2H_O}$ and $tan\theta < \frac{w_R}{L_O}$, the VLC link is not affected by static obstacles, as shown at (3) in Figure 4a.

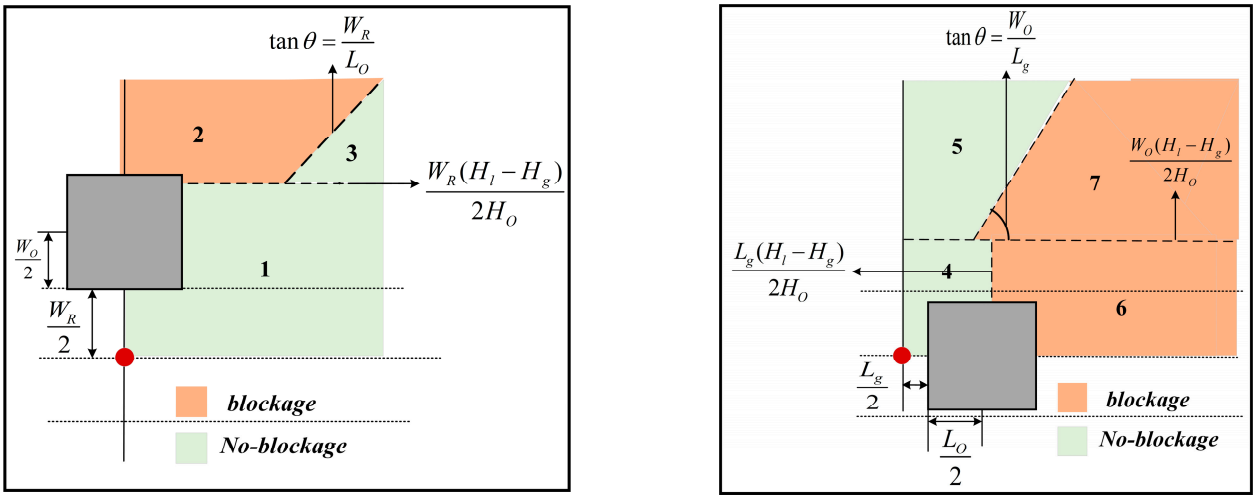

Figure 4. The division of AP area under the influence of different obstacles: (**a**) static obstacle; (**b**) dynamic obstacle.

According to Equation (6), the AP area can be divided into four parts when $D_{go} = \frac{L_g}{2} + \frac{L_O}{2}$. When $D_{gl}sin\theta \leq \frac{W_O(H_l - H_g)}{2H_O}$ *and* $D_{gl}cos\theta < \frac{L_g(H_l - H_g)}{2H_O}$, the VLC link is not affected by dynamic obstacles, as shown at (4) in Figure 4b. When $D_{gl}sin\theta \leq \frac{W_O(H_l - H_g)}{2H_O}$ *and* $D_{gl}cos\theta \geq \frac{L_g(H_l - H_g)}{2H_O}$, the VLC link will be blocked by dynamic obstacles, as shown at (6) in Figure 4b. When $D_{gl}sin\theta > \frac{W_O(H_l - H_g)}{2H_O}$ and $tan\theta > \frac{W_O}{L_g}$, the VLC link is not affected by dynamic obstacles, as shown at (5) in Figure 4b. When $D_{gl}sin\theta > \frac{W_O(H_l - H_g)}{2H_O}$ and $tan\theta \leq \frac{W_O}{L_g}$, the VLC link will be blocked by dynamic obstacles, as shown at (7) in Figure 4b.

4.2. AP-Placement Scheme

In this paper, D_{safe} represents the safe distance between AGV and AP. When the horizontal distance between AGV and AP is less than D_{safe}, the VLC link between AGV and AP is not affected by obstacles. In order to obtain the range of D_{safe}, the effects of both the static obstacle and dynamic obstacle need to be analyzed. Therefore, according to the model analysis results in 4.1, the threshold of D_{safe} can be obtained when the receiver is deployed in the middle of the AGV. D_{safe}^{thr} represents the threshold of D_{safe}. The calculation equation is as follows:

$$D_{safe}^{thr} = \min\left\{\frac{L_g(H_l - H_g)}{2H_O}, \frac{W_O(H_l - H_g)}{2H_O}, \frac{W_R(H_l - H_g)}{2H_O}\right\} \quad (8)$$

D_{AP} represents the distance between APs. When $D_{AP} < 2D_{safe}^{thr}$, for an AGV at any location, the number of APs within its safe distance is not less than 1, as shown in Figure 5a. When $D_{AP} \geq 2D_{safe}^{thr}$, for an AGV in some locations, the number of APs within its safe distance may be 0, as shown in Figure 5b. When the AGV appears in the blocking area, the VLC link between the AGV and the AP may be interrupted by obstacles. Therefore, in order to ensure that the AGV in any location has a non-blocking VLC link, the AP spacing must meet the following condition:

$$D_{AP} < 2D_{safe}^{thr} \tag{9}$$

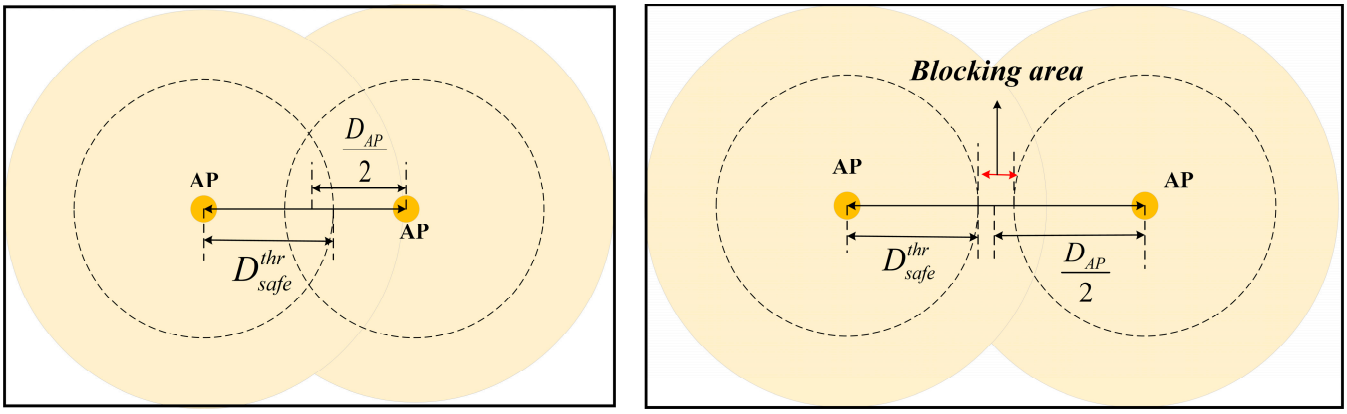

(**a**) (**b**)

Figure 5. Influence of AP Spacing on VLC link: (**a**) $D_{AP} < 2D_{safe}^{thr}$; (**b**) $D_{AP} \geq 2D_{safe}^{thr}$.

According to the above analysis, the AP placement scheme is determined. VLC APs are deployed right above the road. The AP spacing needs to satisfy Equation (9). Under this AP placement, the AGV will establish a connection with the nearest APs. The AGV in any location has a reliable link. The VLC link of the AGV will not be blocked by obstacles.

5. Simulation and Data Analysis

5.1. Model Validity

In order to prove the validity of the link-blockage model, this paper uses another method to judge the state of the VLC link. This method is called the shadow method in this paper. When visible light encounters obstacles, a specific shadow will form, as shown in Figure 6. The shadow area can be obtained by the position of the AP and the obstacle. When the receiver on the AGV is in the shadow area, the VLC link between the AP and the AGV will be blocked. In this paper, the result obtained from the link blockage model is the theoretical value. The result obtained by the shadow method is the simulation value.

In this simulation, a road with a length of 8 m is considered. The AGV is located at the coordinate origin. Static obstacles are deployed on both sides of the road. Dynamic obstacles are deployed on the road. The size of obstacles, the size of AGV, the width of the road and the height of AP are shown in Table 1. The specific position of obstacles is shown in Table 2. The central axis of the road is $y = 0$.

Table 1. Simulation parameters related to working environment.

Parameter	Value	Parameter	Value
L_g	0.84 m	W_g	0.65 m
L_O	0.96 m	W_O	0.96 m
H_g	0.3 m	H_O	2 m
W_R	1 m	H_l	6 m

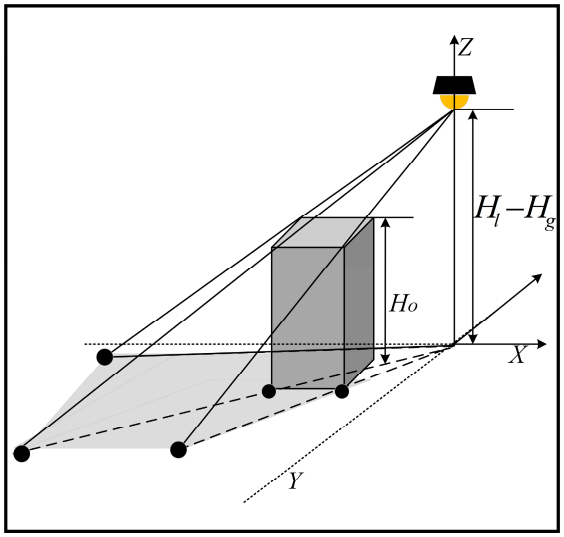

Figure 6. Shadow method.

Table 2. Specific positions of obstacles.

Obstacle	Position	Obstacle	Position
Obstacle-1	(−0.96 m, 0.98 m)	Obstacle-4	(−1 m, 0 m)
Obstacle-2	(0 m, 0.98 m)	Obstacle-5	(1.5 m, 0 m)
Obstacle-3	(0.96 m, 0.98 m)		

According to Equation (5), the link states of APs at different positions under the influence of static obstacles are obtained, as shown in Figure 7a. When $D_{gl}sin\theta \leq \frac{W_R(H_l - H_g)}{2H_O}$, $\gamma_s = 0$ can be obtained by Equation (5). $D_{gl}sin\theta$ is the horizontal distance between AP and the central axis of the road. It can be seen from Figure 7a that when the $D_{gl}sin\theta$ is less than 1.425 m, and the VLC link is not affected by static obstacles. The shelves on both sides of the road are densely arranged. When the $D_{gl}sin\theta$ is greater than 1.425 m, VLC links are easily blocked. It can be seen from Figure 7a that for the AP in $\begin{cases} x_l \in [-4\text{ m}, 4\text{ m}] \\ y_l \in [1.5\text{ m}, 4\text{ m}] \end{cases}$, the VLC link is blocked by static obstacles.

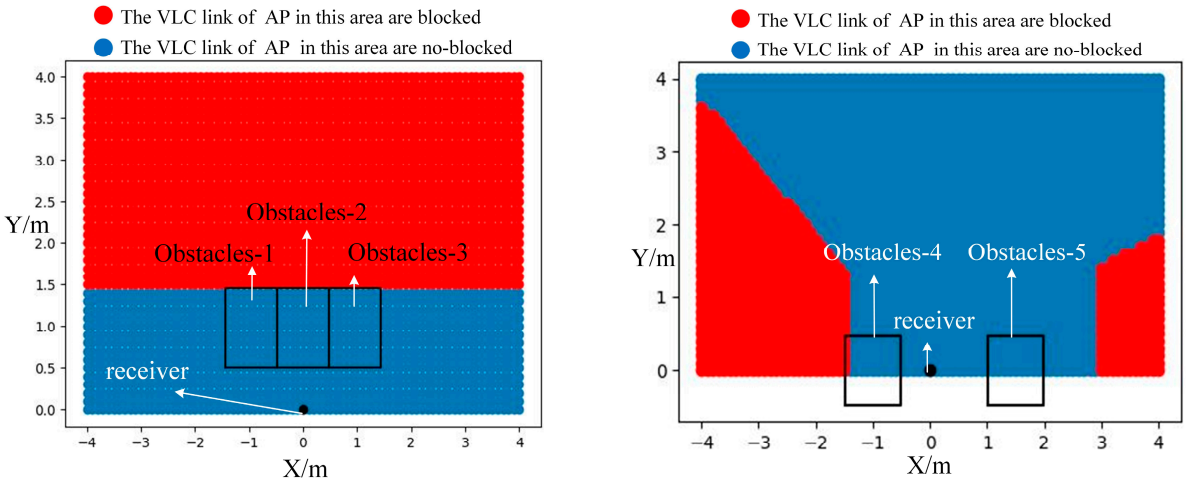

(**a**) (**b**)

Figure 7. Theoretical value of link state obtained by link-blockage model: (**a**) link state of APs under the influence of static obstacles; (**b**) link state of APs under the influence of dynamic obstacles.

According to Equation (6), the link states of APs at different positions under the influence of dynamic obstacles are obtained, as shown in Figure 7b. When $\begin{cases} (x_l - x_g)(x_o - x_g) > 0 \\ D_{gl}sin\theta \leq \frac{W_O(H_l - H_g)}{2H_O} \\ D_{gl}cos\theta \geq \frac{(H_l - H_g)}{H_O}\left|D_{go} - \frac{L_O}{2}\right| \end{cases}$, $\gamma_d = 1$ can be obtained by Equation (6). It can be seen from Figure 7b that for the AP in $x_l \in [-4\text{ m}, 0\text{ m}]$, the VLC link is blocked by obstacle-4 when the $D_{gl}sin\theta$ is less than 1.368 m and the $D_{gl}cos\theta$ is more than 1.482 m. When $\begin{cases} D_{gl}sin\theta > \frac{W_O(H_l - H_g)}{2H_O} \\ \frac{W_O}{2tan\theta} \geq \left|D_{go} - \frac{L_O}{2}\right| \\ (x_l - x_g)(x_o - x_g) > 0 \end{cases}$, $\gamma_d = 1$ can be obtained by Equation (6). It can be seen from Figure 7b that for the AP in $x_l \in [-4\text{ m}, 0\text{ m}]$, the VLC link is blocked by obstacle-4 when the $D_{gl}sin\theta$ is more than 1.368 m, and the angle between the VLC link and the central axis of the road is less than 42.7°.

It can be seen from Figure 7 that when the horizontal distance between AP and the central axis of the road is more than $\frac{W_R(H_l - H_g)}{2H_O}$, the VLC link is easily blocked by static obstacles. Therefore, the AP should be deployed directly above the road. For the AP directly above the road, the blocking probability of the VLC link increases with the increase in the horizontal distance between the receiver and the AP. The blocking probability of the VLC link increases with the decrease in the horizontal distance between the receiver and the obstacle. Therefore, in order to ensure the reliability of the VLC link, AGV should communicate with reliable AP. Reliable AP refers to the AP located right above the road and horizontally close to the AGV. In order to verify the theoretical value, the link states of several typical AP are simulated by the shadow method. The specific positions of APs are shown in Table 3.

Table 3. The specific positions of APs.

AP	Position	AP	Position
AP1	(−3 m, 1 m)	AP5	(2 m, 1 m)
AP2	(−3 m, 2 m)	AP6	(2 m, 2 m)
AP3	(−2 m, 3 m)	AP7	(3.5 m, 1 m)
AP4	(−1 m, 1 m)	AP8	(3.5 m, 2 m)

Under the influence of static obstacles, the shaded areas of different APs are shown in Figure 8. It can be seen from the figure that the receiver is in the shadow of AP2, AP3, AP6 and AP8. The receiver is not in the shadow of AP1, AP4, AP5 and AP7. According to Figure 7, the VLC links of AP2, AP3, AP6 and AP8 are blocked by static obstacles. The VLC links of AP1, AP4, AP5 and AP7 are not blocked by static obstacles. Therefore, the theoretical value is consistent with the simulation value.

Under the influence of dynamic obstacles, the shaded areas of different APs are shown in Figure 9. It can be seen from the figure that the receiver is in the shadow of AP1, AP2 and AP7. The receiver is not in the shadow of AP3, AP4, AP5, AP6 and AP8. According to Figure 7, the VLC link of AP1, AP2 and AP7 are blocked by dynamic obstacles. The VLC link of AP3, AP4, AP5, AP6 and AP8 are not blocked by dynamic obstacles. Therefore, the theoretical value is consistent with the simulation value.

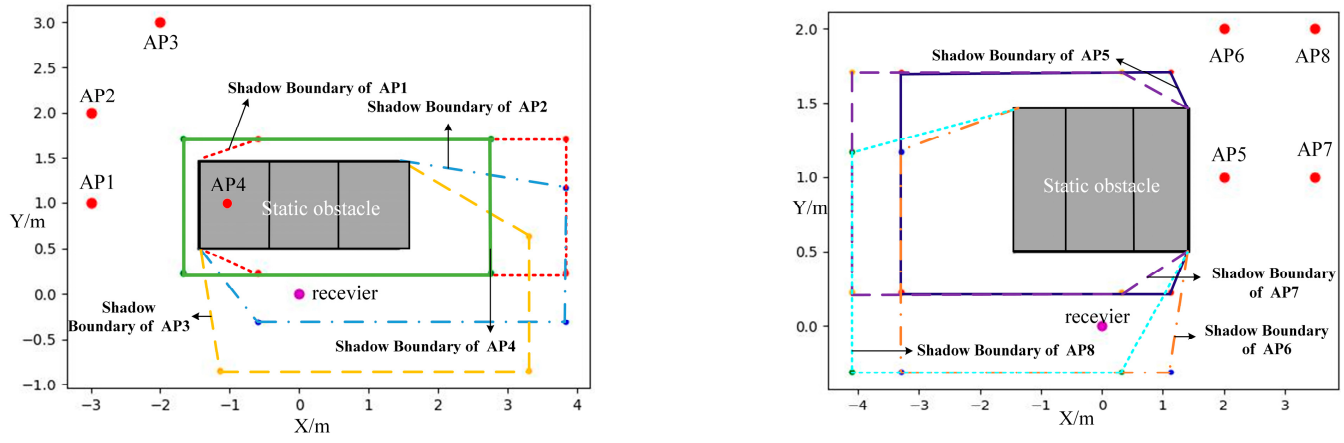

(**a**) (**b**)

Figure 8. Shadows of APs under the influence of static obstacle: (**a**) AP1-AP4; (**b**) AP5-AP8.

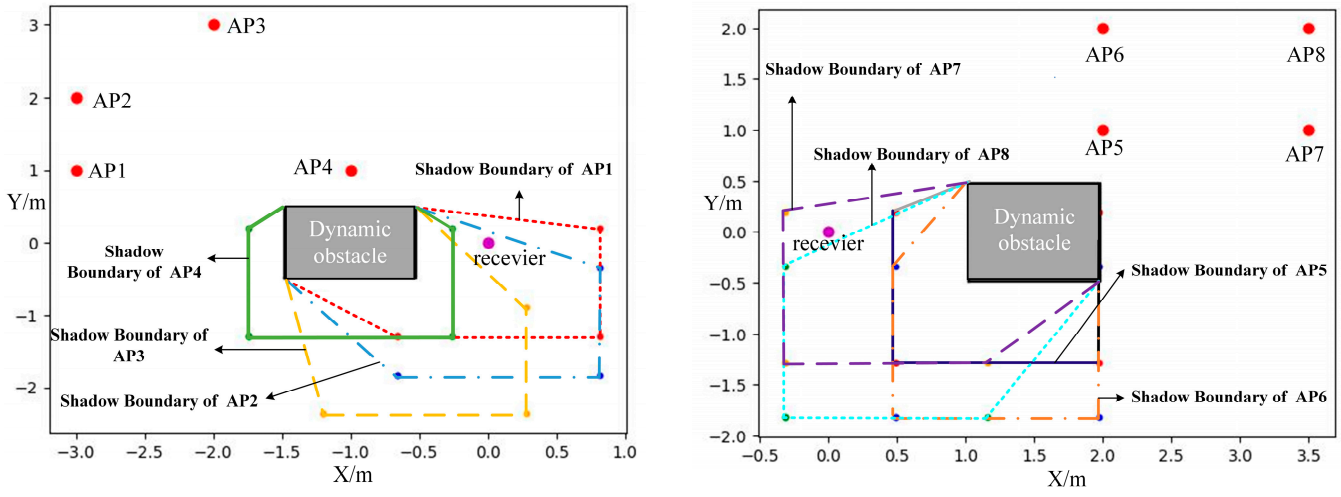

(**a**) (**b**)

Figure 9. Shadows of APs under the influence of dynamic obstacles: (**a**) AP1-AP4; (**b**) AP5-AP8.

5.2. Verification of the Model when Obstacles Are at the Critical Position

The position of the obstacle in this simulation is the same as in Model Analysis 4.1. The position of the receiver is (0 m, 0 m). The position of the static obstacle is (0 m, 0.98 m). The position of the dynamic obstacle is (0.9 m, 0 m). According to model analysis, the AP area can be divided into several parts under the influence of different obstacles. In this simulation, one representative AP is set in each area. The shaded areas of representative APs are shown in Figure 10.

Under the influence of static obstacles, it can be seen from Figure 10 that the receiver is in the shadow of AP3. The receiver is not in the shadow of AP1 and AP4. According to Figure 4a, the AP3 is in the area shown in Figure 4(2). The VLC link between AGV and AP3 is blocked under the influence of static blockage. The AP1 is in the area shown in Figure 4(1). The AP4 is in the area shown in Figure 4(3). The VLC link of AP1 and AP4 are not blocked by static obstacles. Therefore, the theoretical value is consistent with the simulation value. Under the influence of dynamic obstacles, it can be seen from Figure 10 that the receiver is in the shadow of AP2 and AP4. The receiver is not in the shadow of AP1 and AP3. According to Figure 4b, the AP1 is in the area shown in Figure 4(4). The AP3 is in the area shown in Figure 4(5). The VLC link of AP1 and AP3 are not blocked by dynamic obstacles. The AP2 is in the area shown in Figure 4(6). The AP4 is in the area shown in

Figure 4(7). The VLC link of AP2 and AP4 is blocked by dynamic obstacles. Therefore, the theoretical value is consistent with the simulation value.

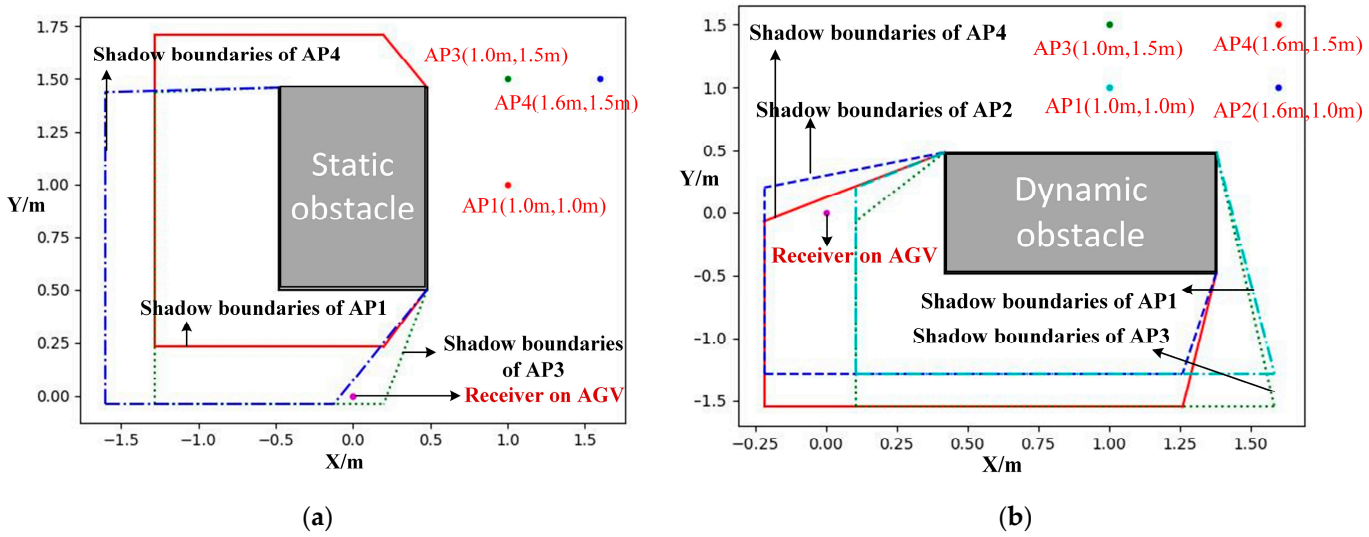

(**a**) (**b**)

Figure 10. Shadows of APs under the influence of obstacle: (**a**) static obstacle; (**b**) dynamic obstacle.

According to Equation (8), the D_{safe}^{thr} is 1.197 m under the current simulation parameters. The shadow area of the APs within D_{safe}^{thr} is calculated, as shown in Figure 11. It can be seen from this figure that the VLC link between the AP and the AGV is not affected by the obstacle when the distance between the AP and AGV is less than 1.197 m.

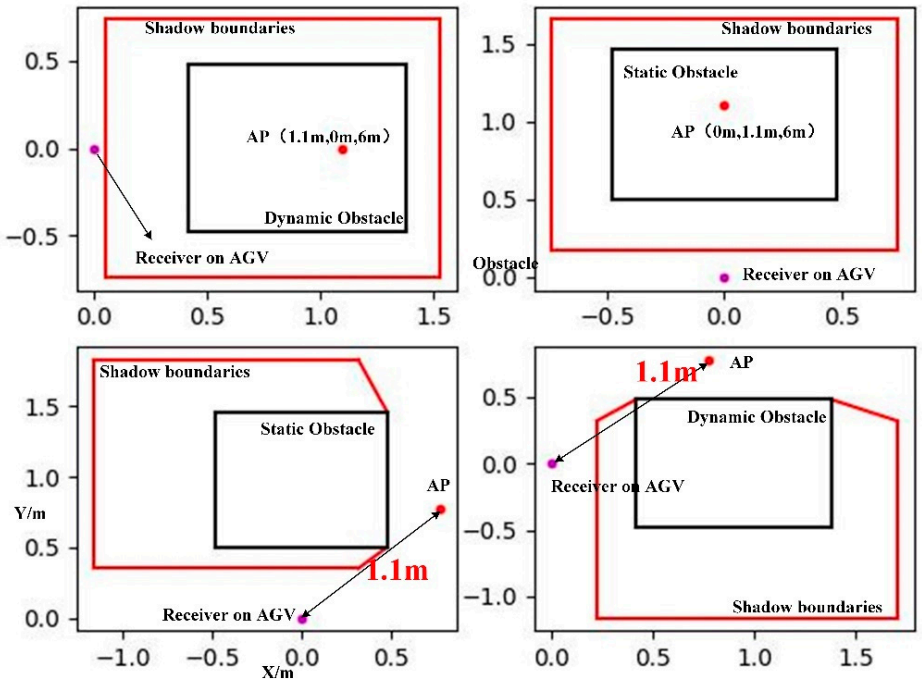

Figure 11. The shadow areas of APs within D_{safe}^{thr}.

5.3. Effectiveness of AP Placement Scheme

According to the link-blockage model, the spacing of the AP placement is obtained to achieve a no-blockage link between the AGV and the VLC AP. In order to prove the effectiveness of the AP placement scheme, the link reliability under different AP spacings is simulated in this paper. This simulation refers to a typical working scenario of AGV in a logistics warehouse. The size of the whole room is 18 m $*$ 13 m $*$ 7 m, as shown

in Figure 12. Static blockages are deployed on all shelves. The number of dynamic obstacles on the road is $N(N = 5, 10, 15, 20, 25)$. APs are deployed right above the road. According to the working environment of AGV, the AP spacing consists of two parts. D_{AP}^{hor} represents the AP spacing in the horizontal direction. D_{AP}^{lon} represents the AP spacing in the longitudinal direction. The setting parameters of AP spacing are: $D_{AP} = \left\{ D_{AP}^{lon} * D_{AP}^{hor} \right\} = \{\{4\text{ m} * 3\text{ m}\}, \{2\text{ m} * 3\text{ m}\}, \{2\text{ m} * 1.5\text{ m}\}, \{1\text{ m} * 1.5\text{ m}\}\}$.

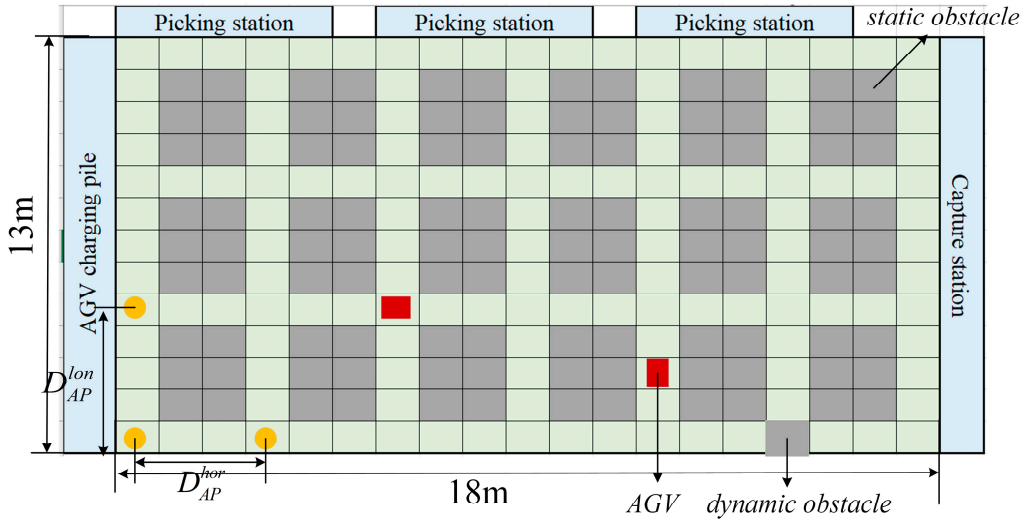

Figure 12. Simulation environment.

For the VLC link between the AGV and the AP, the number of dynamic obstacles, the AP spacing and the AP height will have an impact on link performance. Because APs are deployed directly above the road, static obstacles have less impact on the link. Through the path planning method, N + 1 moving trajectories of AGV are generated. Among the N + 1 trajectories, one trajectory is the moving trajectory of the target AGV. The other N trajectories are the moving trajectories of dynamic obstacles. In order to intuitively display the link performance under the occlusion of obstacles, this paper simulates the outage probability and data rate under different impact factors. In the simulation, the width of the road, the size of the obstacle and the AGV are shown in Table 1. The parameter settings related to the channel are shown in Table 4.

Table 4. Simulation parameters related to VLC channel.

Parameter	Value
Receiver FoV angle, Ψ_c	90°
Half-intensity angle, $\phi_{1/2}$	60°
Refractive index, ζ	1.5
Effective receiving area of the receiver, A	1 cm^2
Gain of optical filter, g_f	1.0
Responsivity of the PD, R_{PD}	0.53 A/W
Noise power spectral density, N	1×10^{-19} W/Hz
Average transmitted optical power, P	30 W
Baseband modulation bandwidth, B	20 MHZ

5.3.1. Average Outage Probability

The average outage probability of the VLC link under different AP heights and AP spacings is shown in Figure 13. As can be seen from the figure, the height of AP, the AP spacing and the number of dynamic obstacles will all affect the outage probability.

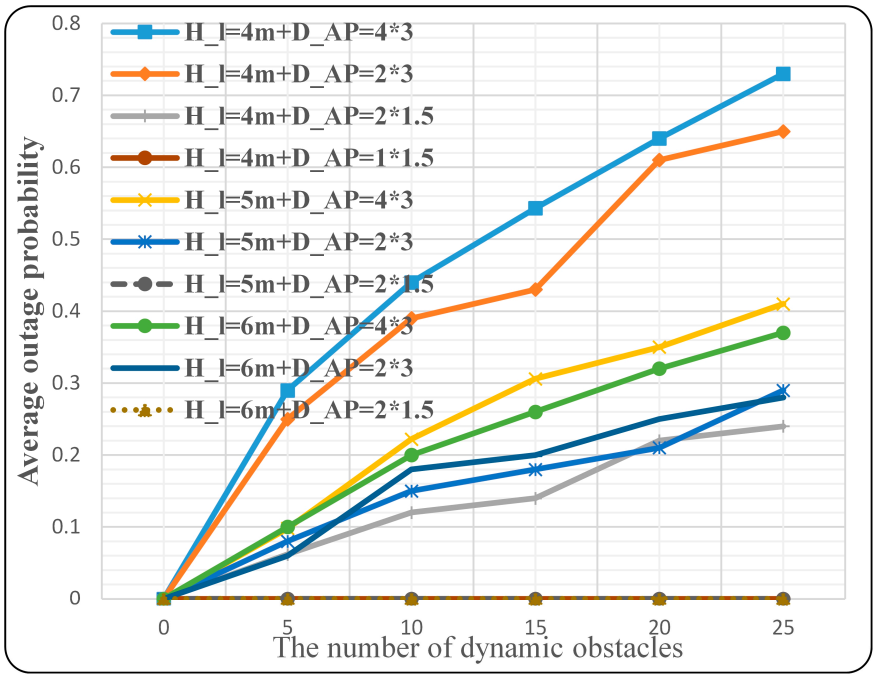

Figure 13. Average outage probability under different AP heights and AP spacings.

Under the same AP height and AP spacing, the outage probability of the VLC link increases with the increase in the number of dynamic obstacles. This is because link blockage is more likely to occur as the number of obstacles increases. The SNR decreases, resulting in an increase in outage probability. Under the same AP spacing and number of dynamic obstacles, the outage probability increases with the decrease in AP height. This is because link blockage is more likely to occur as the AP height decreases. The link outage probability when the AP height is 4 m is significantly greater than that when the AP height is 5 m and 6 m. When the AP height is 4 m, the AP spacing is 4 m * 3 m and the number of dynamic obstacles is 25, the average outage probability is as high as 73%. This shows that when APs are deployed at a low height, and the AP spacing is large, link reliability will be seriously affected. Under the same AP height and number of dynamic obstacles, the link outage probability increases with the increase in the AP spacing. This is because the probability of link blockage will increase with the increase in the AP spacing. When the AP height is 4 m, and the AP spacing is 1 m $*$ 1.5 m, the link outage probability is 0 under different numbers of obstacles. This shows that link outages can be effectively avoided by setting reasonable AP spacing.

It can be seen from Figure 13 that there are three AP placements to ensure the reliability of VLC links. They are: $\{H_l = 4\text{ m}, D_{AP} = 1\text{ m} * 1.5\text{ m}\}$,$\{H_l = 5\text{ m}, D_{AP} = 2\text{ m} * 1.5\text{ m}\}$ and $\{H_l = 6\text{ m}, D_{AP} = 2\text{ m} * 1.5\text{ m}\}$. Under these three AP placements, the average outage probability of the VLC link is 0 under a different number of dynamic obstacles.

5.3.2. Average Data Rate

The average data rate of the VLC link under different AP heights and AP spacings is shown in Figure 14. As can be seen from the figure, the height of AP, the spacings between AP and the number of dynamic obstacles will all affect the data rate.

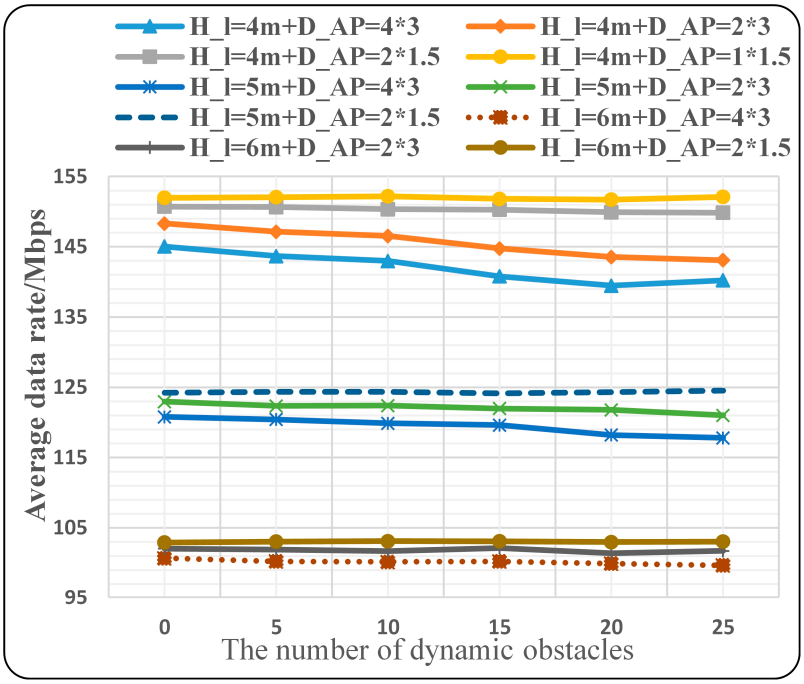

Figure 14. Average data rate under different AP heights and AP spacings.

Under the same number of dynamic obstacles and AP spacing, the average data rate decreases with the increase in the AP height. This is because the channel gain of the receiver decreases with the increase in the AP height. The received power decreases. Therefore, the data rate decreases. Under the same number of dynamic obstacles and AP height, the average data rate decreases with the increase in the AP spacing. This is because the link blockage probability increases with the increase in AP spacing. The SNR decreases under the influence of link blockage. Therefore, the data rate decreases. Under the same AP height and AP spacing, the average data rate decreases with the increase in the number of obstacles. This is because link blockage is more likely to occur as the number of obstacles increases. However, it can be seen from the figure that under the three AP placements of $\{H_l = 4\text{ m}, D_{AP} = 1\text{ m} * 1.5\text{ m}\}$,$\{H_l = 5\text{ m}, D_{AP} = 2\text{ m} * 1.5\text{ m}\}$ and $\{H_l = 6\text{ m}, D_{AP} = 2\text{ m} * 1.5\text{ m}\}$, the data rate is not affected by the number of dynamic obstacles.

5.3.3. Performance Improvement

When the receiver is deployed in the middle of the AGV, there is a safe distance between the AGV and the AP. Given the size of the AGV, the size of the obstacle and the width of the road, the safety distance at different AP heights can be obtained. Thus, the AP spacing can be determined. Through the AP placement scheme proposed in this paper, there is a reliable AP for an AGV at any position. The VLC link between AGV and reliable AP is not affected by obstacles.

According to Equation (8), the D_{safe}^{thr} is 1.197 m when $H_l = 6$ m. The D_{safe}^{thr} is 0.987 m when $H_l = 5$ m. The D_{safe}^{thr} is 0.777 m when $H_l = 4$ m. The comparison between the actual simulation results and the theoretical output results is shown in Table 5. According to the AP-placement scheme proposed in this paper, the AP spacing should be less than 2.394 m when $H_l = 6$ m. According to the simulation results, when $\{H_l = 6\text{ m}, D_{AP} = 2\text{ m} * 1.5\text{ m}\}$, the outage probability of the VLC link is 0 at any number of obstacles. Therefore, when the AP spacing is less than 2.394 m, the reliability of the VLC link can be guaranteed. The comparison results illustrate that the AP-placement scheme proposed in this paper can effectively avoid link interruption.

Table 5. AP placement without link interruption.

AP Height	Theoretical AP Spacing	Actual AP Spacing	Average Data Rate
6 m	$D_{AP} < 2.394$m	2 m ∗ 1.5 m	102 Mbps
5 m	$D_{AP} < 1.974$m	2 m ∗ 1.5 m	124 Mbps
4 m	$D_{AP} < 1.554$m	1 m ∗ 1.5 m	152 Mbps

For the optical link between AGV and AP in the logistics–warehousing VLC network, the aim of this paper is to solve the link interruption caused by link blockage. In this paper, the optimal AP placement needs to ensure the reliability of the VLC link. Under the optimal AP placement, the VLC link of AGV will not be interrupted due to random blockage. The AP placement in Table 5 can meet the uninterrupted requirement. From the point of view of maximizing the average data rate, it can be obtained from Table 5 that the optimal AP placement is $\{H_l = 4\text{ m}, D_{AP} = 1\text{ m} * 1.5\text{ m}\}$. From the point of view of minimizing the number of AP, it can be obtained from Table 5 that the optimal AP placement is $\{H_l = 5\text{ m}, D_{AP} = 2\text{ m} * 1.5\text{ m}\}$ or $\{H_l = 6\text{ m}, D_{AP} = 2\text{ m} * 1.5\text{ m}\}$.

Under optimal AP placement, the influence of the FOV angle on the communication quality of channels in indoor VLC networks will be studied. The average outage probability and average data rate under different FOV angles of the receiver are shown in Figures 15 and 16. Under the optimal AP placement, VLC links are not affected by link blockage. However, the VLC link will be interrupted when $\psi > \Psi_c$. It can be observed from Figure 15 that under the AP placement of $\{H_l = 4\text{ m}, D_{AP} = 1\text{ m} * 1.5\text{ m}\}$, the average outage probability is 0 when $\Psi_c \geq 13°$. Under the AP placement of $\{H_l = 5\text{ m}, D_{AP} = 2\text{ m} * 1.5\text{ m}\}$, the average outage probability is 0 when $\Psi_c \geq 14°$. Under the AP placement of $\{H_l = 6\text{ m}, D_{AP} = 2\text{ m} * 1.5\text{ m}\}$, the average outage probability is 0 when $\Psi_c \geq 11°$.

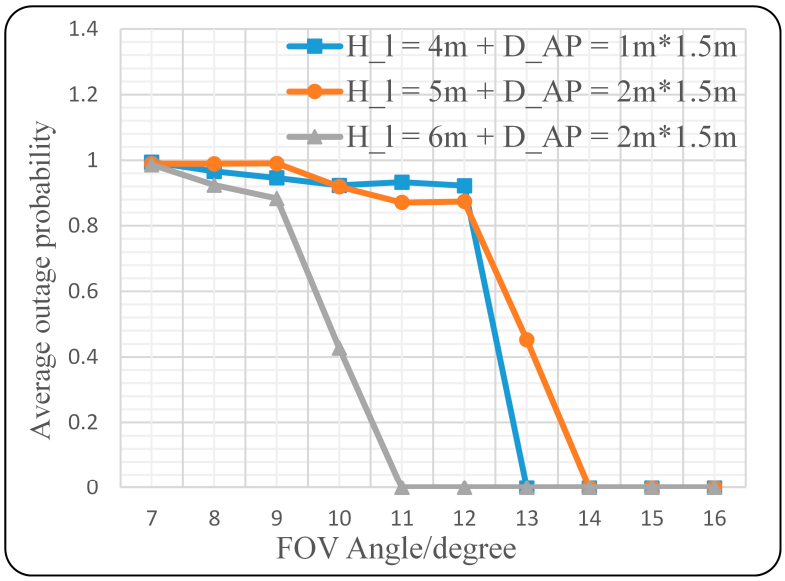

Figure 15. The average outage probability under different FOV angles of receiver.

It can be observed from Figure 16 that the average data rate decreases with the increase in the FOV angle of the receiver. According to the channel model, the channel gain decreases with the increase in the FOV angle. The decrease in received power leads to a decrease in SNR. Therefore, the data rate decreases. In this paper, the performance improvement is to maximize the data rate without link interruption. Therefore, the optimal value of the FOV angle is 13° when the AP placement is $\{H_l = 4\text{ m}, D_{AP} = 1\text{ m} * 1.5\text{ m}\}$. The optimal value of the FOV angle is 14° when the AP placement is $\{H_l = 5\text{ m}, D_{AP} = 2\text{ m} * 1.5\text{ m}\}$. The optimal value of the FOV angle is 11° when the AP placement is $\{H_l = 6\text{ m}, D_{AP} = 2\text{ m} * 1.5\text{ m}\}$.

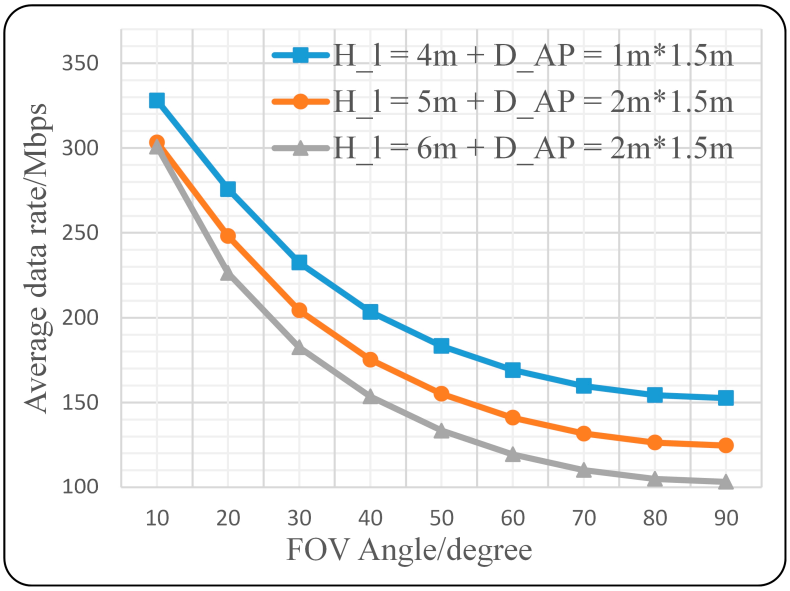

Figure 16. The average data rate under different FOV angles of receiver.

6. Conclusions

In this paper, the blockage problem of the optical link between AGV and AP in the logistics–warehousing VLC network is analyzed. First, a link-blockage model is proposed. Given the position of AGV, AP and obstacle, the link state between AGV and AP can be obtained through this model. Then, an AP-placement scheme based on the link-blockage model is proposed. Under this AP placement, AGVs in any position has a VLC link that is not affected by obstacles. During the process of AGV movement, the reliability of the VLC link can be ensured. Finally, the effectiveness of the link-blockage model is demonstrated by the shadow method. In this paper, the link outage probability and the data rate under different AP heights, AP spacings and the number of obstacles are simulated. Simulation results show that the VLC link can keep uninterrupted under the AP placement proposed in this paper.

Author Contributions: Conceptualization, G.G. and C.G.; methodology, G.G.; software, G.G.; validation, G.G., Y.Z. and Q.H.; formal analysis, G.G. and Y.F.; investigation, G.G.; resources, G.G.; data curation, G.G., Y.Z. and Q.H.; writing—original draft preparation, G.G. and C.G; writing—review and editing, G.G. and C.G; visualization, G.G.; supervision, C.G. and Y.F.; project administration, C.G.; funding acquisition, C.G. All authors have read and agreed to the published version of the manuscript.

Funding: This work was supported in part by the National Key Research and Development Program of China (2021YFB2900801); Science and Technology Commission of Shanghai Municipality (22511100902, 22511100502, 20511102400, 20ZR1420900); 111 Project (D20031).

Institutional Review Board Statement: Not applicable.

Informed Consent Statement: Not applicable.

Data Availability Statement: Not applicable.

Conflicts of Interest: The authors declare no conflict of interest.

References

1. Mapunda, G.A.; Ramogomana, R.; Marata, L.; Basutli, B.; Khan, A.S.; Chuma, J. Indoor Visible Light Communication: A Tutorial and Survey. *Wirel. Commun. Mob. Comput.* **2020**, *2020*, 1–46. [CrossRef]
2. Oyekanlu, E.A.; Smith, A.C.; Thomas, W.P.; Mulroy, G.; Hitesh, D.; Ramsey, M.; Kuhn, D.J.; Mcghinnis, J.D.; Buonavita, S.C.; Looper, N.A.; et al. A Review of Recent Advances in Automated Guided Vehicle Technologies: Integration Challenges and Research Areas for 5G-Based Smart Manufacturing Applications. *IEEE Access* **2020**, *8*, 202312–202353. [CrossRef]
3. Almadani, Y.; Plets, D.; Bastiaens, S.; Joseph, W.; Ijaz, M.; Ghassemlooy, Z.; Rajbhandari, S. Visible Light Communications for Industrial Applications—Challenges and Potentials. *Electronics* **2020**, *9*, 2157. [CrossRef]

4. Jarchlo, E.A.; Eso, E.; Doroud, H.; Zubow, A.; Dressler, F.; Ghassemlooy, Z.; Siessegge, B. FDLA: A Novel Frequency Diversity and Link Aggregation Solution for Handover in an Indoor Vehicular VLC Network. *IEEE Trans. Netw. Serv. Manag.* **2021**, *99*, 1. [CrossRef]
5. Céspedes, M.; Guzmán, B.; Jiménez, V. Lights and Shadows: A Comprehensive Survey on Cooperative and Precoding Schemes to Overcome LOS Blockage and Interference in Indoor VLC. *Sensors* **2021**, *21*, 861. [CrossRef] [PubMed]
6. Singh, A.; Ghatak, G.; Srivastava, A.; Bohara, V.A.; Jagadeesan, A.K. Performance Analysis of Indoor Communication System Using Off-the-Shelf LEDs With Human Blockages. *IEEE Open J. Commun. Soc.* **2021**, *2*, 187–198. [CrossRef]
7. Okine, A.A.; Yun, L.; Sah, M.K. Modeling the Transient Interruption of VLC Downlink by Mobile Blockers. In Proceedings of the 2021 26th IEEE Asia-Pacific Conference on Communications (APCC), Kuala Lumpur, Malaysia, 11–13 October 2021; pp. 29–33.
8. Tang, T.; Shang, T.; Li, Q. Impact of Multiple Shsadows on Visible Light Communication Link. *IEEE Commun. Lett.* **2021**, *25*, 513–517. [CrossRef]
9. Beysens, J.; Wang, Q.; Pollin, S. Exploiting Blockage in VLC Networks Through User Rotations. *IEEE Open J. Commun. Soc.* **2020**, *99*, 1. [CrossRef]
10. Hammouda, M.; Akln, S.; Vegni, A.M.; Haas, H.; Peissig, J. Hybrid RF/LC Systems under QoS Constraints. In Proceedings of the 2018 25th International Conference on Telecommunications (ICT), Saint-Malo, France, 26–28 June 2018; pp. 312–318.
11. Chen, C.; Basnayaka, D.A.; Purwita, A.A.; Wu, X.; Haas, H. Wireless infrared-based LiFi uplink transmission with link blockage and random device orientation. *IEEE Trans. Commun.* **2020**, *69*, 1175–1188. [CrossRef]
12. Dastgheib, M.A.; Beyranvand, H.; Salehi, J.A.; Maier, M. Mobility-Aware Resource Allocation in VLC Networks Using T-Step Look-Ahead Policy. *J. Light. Technol.* **2018**, *36*, 5358–5370. [CrossRef]